Experimental Demonstration of a Tunable Microwave Undulator

Sami Tantawi, Muhammad Shumail,* Jeffery Neilson, Gordon Bowden, Chao Chang,†
Erik Hemsing, and Michael Dunning
SLAC National Accelerator Laboratory, Menlo Park, California 94025, USA
(Received 15 November 2013; published 23 April 2014)

Static magnetic undulators used by x-ray light sources are fundamentally too limited to achieve shorter undulator periods and dynamic control. To overcome these limitations, we report experimental demonstration of a novel short-period microwave undulator, essentially a Thomson scattering device, that has yielded tunable spontaneous emission and seeded coherent radiation. Its equivalent undulator period (λ_u) is 13.9 mm while it has achieved an equivalent magnetic field of 0.65 T. For future-generation light sources, this device promises a shorter undulator period, a large aperture, and fast dynamic control.

DOI: 10.1103/PhysRevLett.112.164802 PACS numbers: 41.60.Cr, 41.60.Ap, 52.59.Rz

X-ray light sources employ permanent magnets that undulate an electron beam to generate radiation. The technology of permanent magnet undulators, which appeared more than 30 years ago [1] for the so-called third-generation light sources [2], is being pushed to its limits to satisfy the requirements of the fourth-generation light sources that are based on self-amplified spontaneous emission (SASE) free-electron lasers driven by linear accelerators (linac) [3,4]. Especially, short-period undulators are required to lower the demand of beam energy. However, permanent magnets are fundamentally limited to achieve shorter periods while maintaining adequate electron beam aperture and field strength [5]. Moreover, fast dynamic polarization control, which is required in the study of magnetic materials and chiral molecules, is not easily achievable with magnetic undulators. These limitations could be overcome using high-power guided microwaves to produce a periodic transverse wiggling field. However, no short-period and high-field implementation of a microwave undulator (MU) has been presented until now.

We present experimental results of a practical MU with an undulator period and a beam aperture of 13.9 and 39 mm, respectively. Its tunable field strength, which can reach 0.65 T, is demonstrated by undulating high-energy electron beams and studying their radiation spectra. We also present the scaling laws of this design, which show that when scaled to shorter undulator periods it maintains a larger beam aperture and higher field strength as compared to the static magnet systems. The azimuthal symmetry of the design allows having any polarization state that can be switched at the rate of hundreds of kilohertz.

The gain length [6] dictated by the experimental setup was not small enough to observe the SASE lasing. The direct laser seeding was also beyond the scope of our experiment. However, we carried out some seeded coherent harmonic generation (SCHG) experiments to show the tunable undulator operation by dynamic selection of the radiated on-axis harmonic of the bunching wavelength.

The principle of MUs to produce synchrotron radiation can be best understood in the inertial frame where the average electron velocity is zero. In this frame, the electron causes Thomson scattering of the Doppler-shifted microwaves. The scattered radiation, Doppler-shifted back to the lab frame, is the highly directional and very high-frequency synchrotron radiation. The stimulated emission in a microwave cavity from a relativistic beam was suggested in 1968 [7]. The first demonstration of an MU came as a ridge waveguide in 1983 [8]. In this configuration, the beam aperture was very small, and the peak undulating fields also appeared on the waveguide surface. Several researchers, motivated to develop new microwave sources, have also studied the MU radiation [9,10]. Recently, a group demonstrated stimulated scattering of a 38-GHz pump wave at TE_{11} mode from a 300-keV high-current electron beam [11]. However, this work provided no means for ensuring field uniformity along the 20-cm-long interaction period. Our motivation to develop MUs came in part from the development of a new rf system that could produce more than 0.5 gigawatt at X-band over a longer pulse length [12]. This, along with the advances in overmoded rf components and systems [13,14], generated the initial discourse on the practicality of the rf undulator [15–17]. Efficient designing of the rf undulator is also essential to fully utilize the high-power rf source. In conventional waveguide structures (see, for example, [8]), the required power, surface fields, and beam aperture scale to impractical values as one goes to the shorter wavelengths while maintaining a reasonable undulator strength. Our device, based on a circular corrugated waveguide operating at the hybrid balanced HE_{11} mode, is a novel, practical demonstration of an MU suitable for light source applications with an order of magnitude higher field than the previous works.

Following [1], the undulator deflecting parameter K is defined in terms of the equivalent undulating magnetic field B_u and the equivalent undulator period λ_u as $K = 93.4\, B_u(\mathrm{T})\lambda_u(\mathrm{m})$. For an MU (see [8–10]), λ_u and

B_u are given as $\lambda_u = \lambda/(1+\lambda/\lambda_g)$ and $B_u = \frac{1}{2}(B_\perp + E_\perp/c)$, where c is the speed of light, λ is the free-space wavelength, λ_g is the guide wavelength, and $B_\perp$ and $E_\perp$ are the peak standing-wave amplitudes of the transverse magnetic and electric fields, respectively.

For the same K parameter and λ_u, the hybrid-balanced HE_{11} mode requires less power and exhibits much higher quality factor and smaller surface fields compared to the fundamental TE_{11} mode. This unique merit of HE_{1n} modes makes it possible to operate the waveguide at extremely high fields at the center without suffering from fatigue due to the surface magnetic fields [18] or breakdown due to the surface electric fields [19]. This also opens the door for the use of superconducting surfaces, as the surface field on the waveguide wall can always be reduced below the quenching limit.

For the HE_{11} mode, the optimal radius $a_{\rm opt}$, which minimizes the required rf power, is given by

$$a_{\rm opt} \approx 0.646\, N_u^{1/3} \lambda_u, \tag{1}$$

where N_u is the number of undulator periods. For $N_u = 100$, $a_{\rm opt} = 3\lambda_u$, which is a much larger aperture than could be realized in any static undulator (SU). For the copper [conductivity: $5.8 \times 10^7 (\Omega m)^{-1}$] cavity with $a = a_{\rm opt}$ and $N_u \gg 1$, we can derive following scaling laws for the required power P and filling-time t_f from the expressions [20] of the HE_{11} mode:

$$P({\rm MW}) \approx 2.46 K^2 N_u^{2/3} \lambda_u^{-1/2} \approx 2.15 B_u^2 N_u^{2/3} \lambda_u^{3/2} \tag{2}$$

$$t_f({\rm ns}) \approx 32.8 N_u \lambda_u^{3/2}, \tag{3}$$

where λ_u is measured in centimeters.

Figure 1(a) shows a cutaway view of our MU that operates at 11.424 GHz. The structure of corrugated guiding walls was optimized using a computer program based on mode-matching technique [21]. The depth and period of corrugation are 6.9 and 11.2 mm, respectively. To reduce the filling time, as required by the available rf source, we chose a radius less than $a_{\rm opt}$ so that with an effective undulator length of 1 m, the aperture size was $2.8\lambda_u$. The ends of the undulator were designed to have suitable field tapering to minimize net transverse drift of the electron beam as it travels through the undulator [22,23]. Without appropriate field tapering, the drift could only be reduced for linear polarization by choosing the right rf phase for the injection of the beam [23,24]. The curved surface is shaped to properly reflect back the diffracted wave to preserve the HE_{11} mode within the overmoded, corrugated waveguide. This design was fabricated as an ultra-high-vacuum device using oxygen-free high-conductivity copper. Using an automated version of quality-factor (Q) measurement from the S parameters [25], the Q of this cavity was measured to be 91 000, which is an order of magnitude higher than that of a typical copper cavity operating at this frequency. To achieve weak coupling without reducing the aperture of the feeding waveguide, we positioned the coupling aperture where the surface electric field exhibits an odd symmetry [Fig. 1(b)] that could only weakly couple to the even symmetry of the fundamental

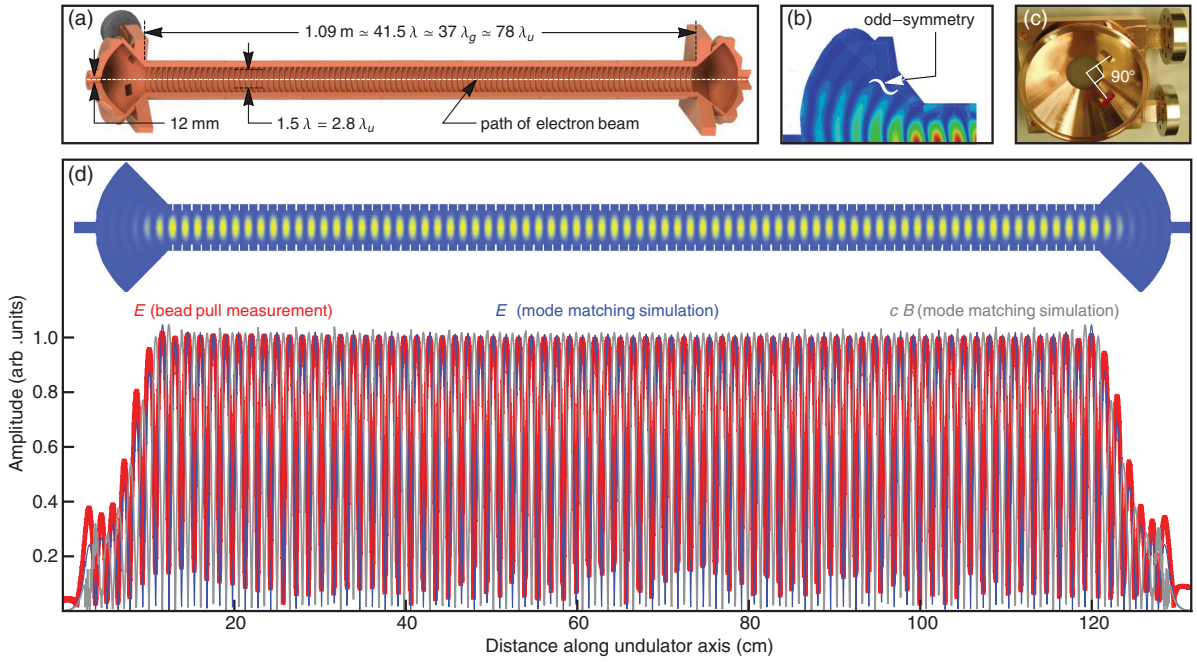

FIG. 1 (color). Design of the undulator with simulated and measured field profiles. (a) Cut-away view of the undulator cavity. (b) Field distribution near a coupling port (simulation with HFSS®, a commercial electromagnetic solver by Ansoft). (c) Implementation of two orthogonal coupling ports. (d) Measured and simulated profiles of the on-axis fields. The inset shows the density plot of the magnitude of the electric field.

mode of the feeding rectangular waveguide. Two couplers separated by 90° in azimuth were implemented [Fig. 1(c)] as the sources of two orthogonal polarizations. Figure 1(d) shows the profiles of on-axis electric (E) and magnetic (B) fields. The E field profile was measured using a bead pull setup, and the data were extracted using perturbation theory as described in [26]. The good agreement between the measured [Fig. 1(d), red] and simulated [Fig. 1(d), blue] results affirms accurate implementation of the undulator. Moreover, the hybrid-balanced nature of the HE_{11} mode is obvious from the same equivalent amplitudes of E [Fig. 1(d), blue] and B [Fig. 1(d), gray] fields.

The MU was tested at the Next Linear Collider Test Accelerator (NLCTA) at the SLAC National Accelerator Laboratory. This facility offers an electron beam of energy ranging from 50 to 120 MeV. In our experiments, the bunch length was about 1 ps (full width at half maximum) for a 30-pC charge. Figure 2 delineates the experimental setup. A 50-MW klystron operating at 11.424 GHz with 1.6-μs (flat-top) pulse fed the MU through a 40-m-long overmoded waveguide. A feed-forward mechanism was employed to compensate for the phase drifts within the klystron pulse. We also shaped the rf pulse to maximize the energy transfer to the MU while maintaining a low level of reflection back to the klystron. To control the rf phase at the injection of the bunch, and hence the transverse bunch drift, we used a phase shifter at the input of the traveling-wave-tube amplifier that fed the klystron. The system was operated at 1, 10, and 60 Hz. The temperature of the MU was regulated at 12.1°C so that the HE_{11} mode was resonant at 11.424 GHz. Whenever heating of the cavity caused a small shift in the resonant frequency (194 kHz/°C), the frequency of rf pulse was changed accordingly by applying appropriate linear phase chirp.

As per our simulation results, the K parameter is related to the stored energy (U) as $U(\text{joules}) = 65\ K^2$. The profile of U and hence K versus time was obtained from the real-time measured data of the incident and reflected powers at the MU (Supplemental Material [27]). The injection timing of the beam was adjusted to coincide with the peak of U and K. The shot-to-shot variation in K was observed to be less than 1%. For this experiment, we used only one coupling port of the MU and hence generated only linearly polarized fields.

A color charge-coupled device camera was set up to receive the snapshots of far-field radiation. To measure the optical spectrum in visible range, another color charge-coupled device camera was used with 300 lines/mm grating setup in front of it. Various optical filters (395, 530, 780 nm, etc.) were used to accurately map the pixel positions to the wavelength. For the ultraviolet (UV) range, a vacuum UV spectrometer was used.

The wavelength of the radiation generated by a linearly polarized undulator is given as follows [1]:

$$\lambda_{\text{rad}}^{(n)} = \lambda_u(1 + K^2/2 + \gamma^2\theta^2)/(2n\gamma^2), \tag{4}$$

where n is the order of harmonic, γ is the electron beam energy measured in units of electron mass (≈ 0.511 MeV), and θ is the small angular distance from the axis of the undulator to the point of observation. The fundamental wavelength of on-axis radiation $\lambda_{\text{rad}}^{(1)}$ was calculated by correlating the measured and theoretical spectra.

Figure 3(a) presents the measured spectra for various values of K at 70.3 MeV. The theoretically calculated spectrum for $K = 0.69$ is also shown for reference. Figure 3(b) shows fundamental wavelength of on-axis radiation $\lambda_{\text{rad}}^{(1)}$ versus K for beam energies of 53.5 MeV [Fig. 3(b), red] and 70.3 MeV [Fig. 3(b), blue]. In Fig. 3, the values of K were obtained by best fitting the values of $\lambda_{\text{rad}}^{(1)}$ obtained from the spectrum measurements to the values of K obtained from rf measurements. The measured data closely match the theoretical predictions of Eq. (4), which

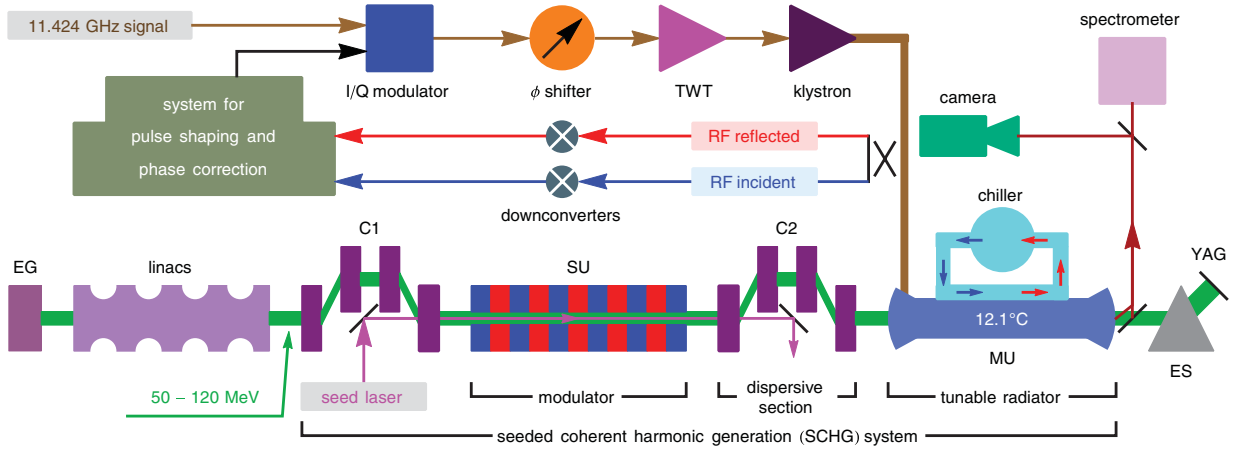

FIG. 2 (color). Schematic layout of microwave undulator demonstration experiment at NLCTA, SLAC. EG: electron gun, C1: bypass chicane to introduce seed laser, SU: static undulator, C2: chicane used for spatial bunching when required, MU: microwave undulator, ES: energy spectrometer for electron beam, YAG: yttrium aluminum garnet screen.

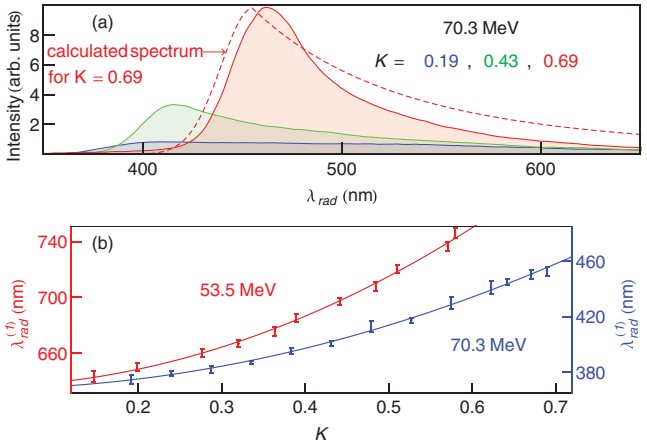

FIG. 3 (color). Demonstration of tunable undulator operation. (a) Spectra for various K. (b) Fundamental wavelength of on-axis radiation vs K for two beam energies. Each point with an error bar indicates a mean and standard deviation obtained from 10 to 100 data snapshots. The solid lines are plots obtained from Eq. (4) where $n = 1$ and $\theta = 0$.

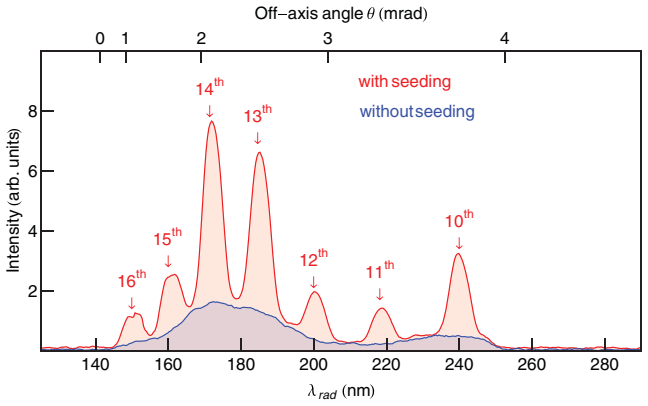

FIG. 4 (color). SCHG. The spectra with and without seeding are shown as red and blue plots, respectively. The location of various harmonics of 2.4-μm bunching are indicated with arrows (beam energy = 120 MeV, $K_{SU} = 2.76$, $\lambda_{SU} = 5.5$ cm, $K_{MU} = 0.49$, $\lambda_{MU} = 1.39$ cm).

are plotted as solid lines. The main sources of uncertainty in the calculation of radiation wavelength are the rf power measurements that determine the K parameter and the beam energy measurements.

In these experiments, we typically had beam current = 30 A, rms beam size = 0.2 mm, beam energy = 70 MeV, and $K = 0.6$, which yielded a one-dimensional gain length [6] of about 0.5 m, half the undulator length. It was not possible to observe the SASE lasing in two gain lengths. Also, the routing of the laser beam in the facility could not be changed to allow for direct laser seeding experiment, in which case some gain could be observed. However, we carried out some SCHG experiments to demonstrate the tunability of our undulator. As shown in Fig. 2, the setup for SCHG experiments includes a seed laser, a SU, and a chicane (C2), which were used along with the MU. We use the symbols K_{SU} or K_{MU} and λ_{SU} or λ_{MU} to distinguish the K and λ_u of SU and MU, respectively.

The results of tunable SCHG are shown in Fig. 4. The beam energy was fixed to 120 MeV, and K_{MU} was kept at 0.49 so that $\lambda_{rad}^{(1)}$ was 141 ± 5 nm according to Eq. (4). The spectrum obtained without seeding spanned 145–250 nm (Fig. 4, blue). Note that the intensity axis is not calibrated to cater for the response of optics for various wavelengths. For seeding, we used a 2.4-μm laser, derived from an optical parametric amplification system. We had SU with $K_{SU} = 2.76$ and $\lambda_{SU} = 5.5$ cm so that its fundamental radiation wavelength was also 2.4 μm. The electrons bunched at 2.4 μm gave rise to the strong coherent radiation at the bunching harmonics that overlapped with the spectrum of MU (Fig. 4, red). By changing K_{MU}, we could shift the spectrum of MU and hence pick other harmonics of bunching. Such dynamic selection of harmonics is not possible with conventional SUs. A similar SCHG experiment was also carried out with a commercial Ti:sapphire 800-nm seed laser (Supplemental Material [28]).

We have demonstrated a short-period, large-aperture undulator based on a microwave resonator with low surface fields. As verified by the spectrum measurements of radiation, this device can achieve K parameter of order 1. Moreover, the K parameter can be controlled dynamically to tune the radiation wavelength. The discussion about the experimental setup and the gain length of our device will help the researchers interested in using this device for advanced applications. We have also provided the scaling laws of our design, which show that an efficient implementation with even shorter undulator periods is possible. This design is also amenable to superconductor implementation requiring a relatively low power source, which would allow efficient use of the device in storage-ring-based light sources and could lead to the next generation of fast-tunable light sources.

We are thankful to Claudio Pellegrini for the initial encouragement, Valery Dolgashev for the useful discussions, the fabrication facilities staff of the SLAC National Accelerator Laboratory for precise machining of the MU, Carsten Hast for facilitating our experiment at the NLCTA at SLAC, and Stephen Weathersby for assisting with beam operations. This project was funded by U.S. Department of Energy under Contract No. DE-AC02-76SF00515 and the DARPA AXiS program.

*shumail@slac.stanford.edu
†Present address: Laboratory of Science and Technology on High Power Microwave, NINT, Xi'an, China, 710024

[1] K. Halbach, J. Chin, E. Hoyer, H. Winick, R. Cronin, J. Yang, and Y. Zambre, IEEE Trans. Nucl. Sci. **28**, 3136 (1981).

[2] H. Winick, in *16th International Conference on X-ray and Inner-Shell Processes* (North-Holland, Debrecen, Hungary, 1994), p. 112.
[3] P. Emma, R. Akrel, J. Arthur, R. Bionta, C. Bostedt, and J. Bozek, Nat. Photonics **4**, 641 (2010).
[4] T. Ishikawa, H. Aoyagi, T. Asaka, Y. Asano, N. Azumi, and T. Bizen, Nat. Photonics **6**, 540 (2012).
[5] *Synchrotron Radiation Instrumentation, AIP Conference Proceedings*, edited by T. Warwick, J. Arthur, H. A. Padmore, and J. Stöhr (American Institute of Physics, San Francisco, CA, 2004), Vol. **705**.
[6] Z. Huang and K.-J. Kim, Phys. Rev. ST Accel. Beams **10**, 034801 (2007).
[7] R. Pantell, G. Soncini, and H. Puthoff, IEEE J. Quantum Electron. **4**, 905 (1968).
[8] T. Shintake, Proc. SPIE Int. Soc. Opt. Eng. **0582**, 336 (1986).
[9] T. Tran, B. Danly, and J. Wurtele, IEEE J. Quantum Electron. **23**, 1578 (1987).
[10] B. Danly, G. Bekefi, R. Davidson, R. Temkin, T. Tran, and J. Wurtele, IEEE J. Quantum Electron. **23**, 103 (1987).
[11] A. Reutova, M. Ulmaskulov, A. Sharypov, V. Shpak, S. Shunailov, M. Yalandin, V. Belousov, N. Ginzburg, G. Denisov, I. Zotova, R. Rozental, and A. Sergeev, J. Exp. Theor. Phys. Lett. **82**, 263 (2005).
[12] S. G. Tantawi, C. D. Nantista, V. A. Dolgashev, C. Pearson, J. Nelson, K. Jobe, J. Chan, K. Fant, J. Frisch, and D. Atkinson, Phys. Rev. ST Accel. Beams **8**, 042002 (2005).
[13] S. G. Tantawi, C. D. Nantista, G. B. Bowden, K. S. Fant, N. M. Kroll, A. E. Vlieks, Y.-H. Chin, H. Hayano, V. F. Vogel, and J. Neilson, Phys. Rev. ST Accel. Beams **3**, 082001 (2000).
[14] S. G. Tantawi, C. Nantista, N. Kroll, Z. Li, R. Miller, R. Ruth, P. Wilson, and J. Neilson, Phys. Rev. ST Accel. Beams **5**, 032001 (2002).
[15] C. Pellegrini, in *27th FEL Conference Proceedings* (Joint Accelerator Conference Website, Stanford, CA, 2005).
[16] S. Tantawi, V. Dolgashev, C. Nantista, C. Pellegrini, J. Rosenzweig, and G. Travish, in *27th FEL Conference Proceedings* (Joint Accelerator Conference Website, Stanford, CA, 2005).
[17] M. Yeddulla, H. Geng, Z. Ma, Z. Huang, and S. Tantawi, in *Proc. EPAC2008* (European Physical Society Accelerator Group, Genoa, Italy, 2008).
[18] L. Laurent, S. Tantawi, V. Dolgashev, C. Nantista, Y. Higashi, M. Aicheler, S. Heikkinen, and W. Wuensch, Phys. Rev. ST Accel. Beams **14**, 041001 (2011).
[19] V. Dolgashev, S. Tantawi, Y. Higashi, and B. Spataro, Appl. Phys. Lett. **97**, 171501 (2010).
[20] M. Shumail, G. Bowden, C. Chang, J. Neilson, and S. Tantawi, in *Proc. IPAC2011* (European Physical Society Accelerator Group, San Sebastián, Spain, 2011), p. 3326.
[21] J. Neilson, P. Latham, M. Caplan, and W. Lawson, IEEE Trans. Microwave Theory Tech. **37**, 1165 (1989).
[22] C. Chang, J. M. Neilson, C. Pellegrini, M. Shumail, and S. G. Tantawi, in *Proc. IPAC2012* (IEEE, New Orleans, LA, 2012), p. 753.
[23] C. Chang, M. Shumail, S. Tantawi, J. Neilson, and C. Pellegrini, Appl. Phys. Lett. **101**, 161102 (2012).
[24] M. Shumail, G. Bowden, C. Chang, J. Neilson, and S. Tantawi, in *AIP Conf. Proc.* (American Institute of Physics, Austin, TX, 2012), Vol. **1507**, p. 752.
[25] E. L. Ginzton, *Microwave Measurements* (*McGraw-Hill Book Company*, New York, 1957), Chap. 9.
[26] C. Steele, IEEE Trans. Microwave Theory Tech. **14**, 70 (1966).
[27] See Supplemental Material at http://link.aps.org/supplemental/10.1103/PhysRevLett.112.164802 for the details on the calculation of the stored energy and the K parameter.
[28] See Supplemental Material at http://link.aps.org/supplemental/10.1103/PhysRevLett.112.164802 for the results of the SCHG experiment with a 800-nm seed laser.